

Stability of discrete solitons in the presence of parametric driving

H. Susanto,¹ Q. E. Hoq,² and P. G. Kevrekidis¹

¹Department of Mathematics and Statistics, University of Massachusetts, Amherst, Massachusetts 01003-4515, USA

²Department of Physical and Biological Sciences, Western New England College, Springfield, Massachusetts, 01119, USA

(Received 2 May 2006; published 4 December 2006)

In this Brief Report, we consider parametrically driven bright solitons in the vicinity of the anticontinuum limit. We illustrate the mechanism through which these solitons become unstable due to the collision of the phase mode with the continuous spectrum, or eigenvalues bifurcating thereof. We show how this mechanism typically leads to *complete destruction* of the bright solitary wave.

DOI: 10.1103/PhysRevE.74.067601

PACS number(s): 05.45.Yv

I. INTRODUCTION

In the past few years, differential-difference dispersive equations where the evolution variable is continuum but the spatial variables are discrete, have been the focus of intense research efforts [1]. The key reason for the increasing interest in this research direction can be attributed to the wide range of pertinent applications ranging, from, e.g., the spatial dynamics of optical beams in coupled waveguide arrays in nonlinear optics [2], to the temporal evolution of Bose-Einstein condensates (BECs) in deep, optically induced, lattice potentials in condensed matter physics [3], or even to the DNA double strand in biophysics [4] among others.

One of the key models that has emerged in all of the above settings, either as describing, e.g., the envelope wave of the electric field in the optical setting [5], or describing the wavefunction at the nodes of the optical lattice in BECs [6], is the discrete nonlinear Schrödinger (DNLS) equation. This prototypical lattice model features a dispersive coupling between nearest neighbors, and a cubic onsite nonlinearity.

The above spatially discrete model bears a number of interesting similarities and differences, in comparison with its continuum sibling, the famous (integrable in 1-spatial dimension) nonlinear Schrödinger equation (NLS) [7]. One of the key differences is the breaking of one of the important invariances of the NLS model, namely of the translational invariance that is responsible for momentum conservation in that setting. On the contrary, the discrete model carries an integer-shift invariance. This has some important implications for the nature of the solutions of the discrete model. In fact, it was realized through perturbative calculations [8] and subsequently more rigorously justified [9] that the principal (single-humped solitary wave) solutions of the latter model can only be centered on a lattice site or between two lattice sites. In the continuum case, the center of the solution is a free parameter due to the continuum invariance.

On the other hand, one of the important similarities of the discrete model to the continuum one is the presence of the so-called phase or gauge invariance (which is associated with the overall freedom of selecting the solution's phase). The conservation law related to this invariance is the one of the L^2 (respectively, ℓ^2) norm, or "mass" of the solution. This invariance is the main focal point of the present work. In particular, we introduce, arguably, the simplest possible perturbation that breaks the relevant invariance, in the form of a parametric drive. The relevance of such a term involving a perturbation proportional to the complex conjugate of the

field has been discussed in a variety of earlier works (see, e.g., [10] and references therein). A specific physical setting where this type of perturbation arises can be found by looking at the envelope equation of a system of parametrically driven (undamped) coupled torsion pendula as discussed in [11] (with the difference that the envelope wave expansion should be performed in a genuinely discrete setting similarly to [12] rather than near the continuum limit as in [11]). The aim of this exposition is to examine how the breaking of this invariance results in an eigenvalue that bifurcates from the origin of the spectral plane, when linearizing around the most fundamental, solitary wave solution. We argue (analytically and support numerically) that this eigenvalue can lead to an instability of the solitary wave for an isolated value of the parametric drive even at the so-called anticontinuum limit where lattice sites are uncoupled. For nonvanishing couplings, the same eigenvalue leads to an interval of parametric instabilities in the two-parameter space (of parametric drive versus intersite coupling) that we explore analytically and numerically. Within this interval, we also elucidate the typical behavior of the solitary wave solutions, using direct numerical simulations of relevant unstable waveforms.

Our presentation will be structured as follows. In the next section, we present our analytical setup and perturbative results. Then, we compare our analytical findings with the results of numerical computations. Finally, we summarize our findings and present our conclusions, as well as motivate some questions for future study.

II. SETUP AND PERTURBATION ANALYSIS

The model we consider is the perturbed (i.e., parametrically driven) discrete nonlinear Schrödinger equation of the form

$$i\dot{\phi}_n = -C\Delta_2\phi_n - |\phi_n|^2\phi_n + \Lambda\phi_n + \gamma\overline{\phi_n}, \quad (1)$$

where C is the coupling constant between two adjacent sites of the lattice, $\Delta_2\phi_n = (\phi_{n+1} - 2\phi_n + \phi_{n-1})$ is the discrete Laplacian, Λ is the propagation constant in optics or the chemical potential in BECs, and γ is the strength of the parametric drive.

We focus our attention on a standing wave profile so that ϕ_n is time independent. In this case, ϕ_n satisfies

$$-C\Delta_2\phi_n - \phi_n^3 + \Lambda\phi_n + \gamma\phi_n = 0. \quad (2)$$

In the uncoupled [or so-called anticontinuum (AC)] limit of $C=0$, the solution of (2) is $\phi_n=0, \pm\sqrt{\Lambda+\gamma}$. We examine here the most fundamental single-hump solitary wave solutions which in the AC limit emanate from a single-site excitation of the form

$$u_n^0=0, \quad n \neq 0, \quad u_0^0=\sqrt{\Lambda+\gamma}. \quad (3)$$

The continuation of (3) for small coupling C can be calculated analytically through a perturbative expansion. By substituting into the steady state equation (2) $u_n=u_n^{(0)}+Cu_n^{(1)}+C^2u_n^{(2)}+\dots$, one can calculate that up to order $\mathcal{O}(C^2)$

$$u_n=\begin{cases} \sqrt{\Lambda+\gamma}+C/\sqrt{\Lambda+\gamma}, & n=0, \\ C/\sqrt{\Lambda+\gamma}, & n=-1,1, \\ 0, & n \text{ otherwise.} \end{cases} \quad (4)$$

To examine the stability of the discrete solitary waves of the form of Eq. (4), we introduce the following linearization ansatz $\phi_n=u_n+\delta\epsilon_n$. Substituting into (1) yields the following linearized equation to $\mathcal{O}(\delta)$:

$$i\dot{\epsilon}_n=-C\Delta_2\epsilon_n-2|u_n|^2\epsilon_n-u_n^2\bar{\epsilon}_n+\Lambda\epsilon_n+\gamma\bar{\epsilon}_n. \quad (5)$$

Writing $\epsilon_n(t)=\eta_n+i\xi_n$ and assuming that u_n is real, Eq. (5) gives (see, e.g., [13])

$$\begin{pmatrix} \dot{\eta}_n \\ \dot{\xi}_n \end{pmatrix}=\begin{pmatrix} 0 & \mathcal{L}_+(C) \\ -\mathcal{L}_-(C) & 0 \end{pmatrix}\begin{pmatrix} \eta_n \\ \xi_n \end{pmatrix}=\mathcal{H}\begin{pmatrix} \eta_n \\ \xi_n \end{pmatrix}, \quad (6)$$

where the operators $\mathcal{L}_-(C)$ and $\mathcal{L}_+(C)$ are defined as $\mathcal{L}_-(C)\equiv-C\Delta_2-(3u_n^2-\Lambda-\gamma)$ and $\mathcal{L}_+(C)\equiv-C\Delta_2-(u_n^2-\Lambda+\gamma)$. The stability of u_n is then determined by the eigenvalues of \mathcal{H} .

Let the eigenvalues of \mathcal{H} be denoted by $i\omega$, which implies that u_n is stable if $\text{Im}(\omega)=0$. Because (6) is linear, we can eliminate one of the eigenvectors, for instance ξ_n , from which we obtain the following eigenvalue problem:

$$\mathcal{L}_+(C)\mathcal{L}_-(C)\eta_n=\omega^2\eta_n=\Omega\eta_n. \quad (7)$$

As before, we expand the eigenvector η_n and the eigenvalue Ω as $\eta_n=\eta_n^{(0)}+C\eta_n^{(1)}+\mathcal{O}(C^2)$ and $\Omega=\Omega^{(0)}+C\Omega^{(1)}+\mathcal{O}(C^2)$. Substituting into Eq. (7) and identifying coefficients for consecutive powers of the small parameter C yields

$$[\mathcal{L}_+(0)\mathcal{L}_-(0)-\Omega^{(0)}]\eta_n^{(0)}=0, \quad (8)$$

$$[\mathcal{L}_+(0)\mathcal{L}_-(0)-\Omega^{(0)}]\eta_n^{(1)}=f, \quad (9)$$

with

$$f=[-(\Delta_2+2u_n^{(0)}u_n^{(1)})\mathcal{L}_-(0)-\mathcal{L}_+(0)(\Delta_2+6u_n^{(0)}u_n^{(1)})+\Omega^{(1)}]\eta_n^{(0)}. \quad (10)$$

First, let us consider the order $\mathcal{O}(1)$ equation (8). A simple analysis shows that there are only two eigenvalues, i.e., $\Omega^{(0)}=\Lambda^2-\gamma^2$ and $\Omega^{(0)}=4(\Lambda+\gamma)\gamma$. $\Omega^{(0)}=\Lambda^2-\gamma^2$ has infinite multiplicity and is related to the phonon band of linear excitations (mathematically, the so-called continuous spectrum) that will be discussed later. Therefore, our interest is in $\Omega^{(0)}=4(\Lambda+\gamma)\gamma$ that has the normalized eigenvector $\eta_n^{(0)}=0$,

$n \neq 0$ and $\eta_0^{(0)}=1$. This eigenvalue is the formerly zero eigenvalue due to the phase or gauge invariance of the DNLS equation *in the absence of parametric driving*, i.e., its invariance with respect to an arbitrary rotation of the phase (cf. for both types of eigenvalues with the discussion in Sec. II B of [13]).

The continuation of the eigenvalue $\Omega^{(0)}=4(\Lambda+\gamma)\gamma$ when the coupling C is turned on can be calculated from Eq. (9). Due to the corresponding eigenvector having $\eta_n^{(0)}=0$ for $n \neq 0$, we only need to consider the site $n=0$. In this case, $f=-8\gamma+\Omega^{(1)}$. The solvability condition of Eq. (9) using, e.g., the Fredholm alternative requires $f=0$ from which we immediately obtain that $\Omega^{(1)}=8\gamma$. Hence, the smallest eigenvalue of a one-site discrete soliton solution of Eq. (1) is

$$\Omega=4(\Lambda+\gamma)\gamma+8\gamma C+\mathcal{O}(C^2), \quad (11)$$

or

$$\omega=\pm 2\sqrt{(\Lambda+\gamma)\gamma}\pm 2\frac{\gamma}{\sqrt{(\Lambda+\gamma)\gamma}}C+\mathcal{O}(C^2). \quad (12)$$

If $\gamma=\mathcal{O}(C)$, Eq. (12) becomes

$$\omega=\pm 2\sqrt{\Lambda\gamma}\sqrt{C}+\mathcal{O}(C). \quad (13)$$

Next, we have to proceed with calculating the continuous spectrum of the operator $\mathcal{L}_+(C)\mathcal{L}_-(C)$ [(7)]. When $C=0$, the entire phonon band lies at $\Omega=\Lambda^2-\gamma^2$ as was mentioned before. When C is increased, the linear excitations start forming a “true band” (which expands as $C \uparrow$). Using a plane wave expansion $\eta_n=ae^{i\kappa n}+be^{-i\kappa n}$ yields the dispersion relation

$$\Omega=(\Lambda+\gamma+2C-2C\cos\kappa)(\Lambda-\gamma+2C-2C\cos\kappa). \quad (14)$$

Hence, the continuous band lies between $\Omega_L=\Lambda^2-\gamma^2$ (when $\kappa=0$) and $\Omega_U=\Lambda^2-\gamma^2+8C(\Lambda+2C)$ (when $\kappa=\pi$).

For small γ , the instability of a one-site solitary wave of (1) is caused by the collision of the phase mode eigenvalue (11) with an eigenvalue bifurcating from Ω_L . However, here we assume that the bifurcating eigenvalue does not move very fast in the spectral plane such that it can be represented by Ω_L . For large γ , the instability is due to the collision of the phase mode eigenvalue and Ω_U . Equating those quantities will give the critical γ as a function of the coupling constant C (i.e., all intermediate γ 's will be resonantly unstable due to the collision of the phase eigenvalue with the phonon band), through

$$\gamma_{\text{cr}}^1=-\frac{2}{5}\Lambda-\frac{4}{5}C+\frac{1}{5}\sqrt{9\Lambda^2+16C(\Lambda+C)}, \quad (15)$$

$$\gamma_{\text{cr}}^2=-\frac{2}{5}\Lambda-\frac{4}{5}C+\frac{1}{5}\sqrt{9\Lambda^2+56C\Lambda+96C^2}. \quad (16)$$

The two approximate γ_{cr}^i above coincide at $C=0$ and $\gamma^*=(\sqrt{2}-1)/2 \approx 0.2071$. Notice that at that level the relevant calculation is analytically exact (i.e., there is no approximation and the single-site excitation will be unstable for $C=0$ only for $\gamma=\gamma^*$). While we have not seen this result (of the critical γ^*) for the single oscillator published elsewhere, it is rather straightforward to extract from settings and techniques

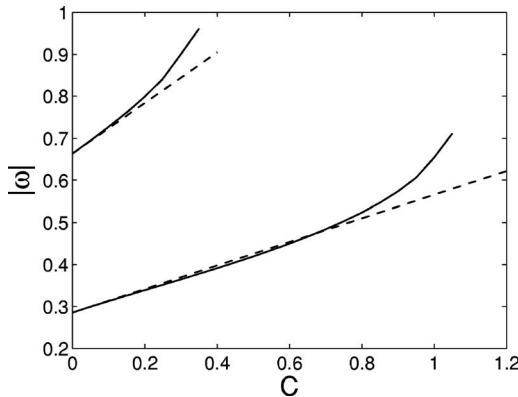


FIG. 1. The smallest eigenvalue for two values of γ , namely $\gamma=0.02$ and $\gamma=0.1$. The dashed lines are the approximate analytical estimate of the relevant frequency from Eq. (12). The lower curves correspond to $\gamma=0.02$.

discussed earlier such as the setting of [10] and the analysis of [14].

III. NUMERICAL RESULTS

We now proceed to test our analytical results for the parametrically driven equation numerically. We start by examining the validity of our analytical prediction for the eigenfrequency corresponding to the phase mode which bifurcates from $\omega=0$ because of the presence of the parametric drive according to the expression (12). Figure 1 shows this prediction as a function of C for two different values of γ . Clearly, the prediction is fairly accurate for small C and its range of validity is wider for smaller values of γ .

We now turn to the examination of the two-parameter plane of the parametric drive γ versus the coupling strength C . Figure 2 provides a full description of the dynamics of the parametrically driven DNLS model regarding the intervals of stability/instability of the most fundamental, single-hump solitary wave solution of the model. The solid lines show the numerically obtained separatrices between the stable and unstable parametric regimes of the model, while the dashed and

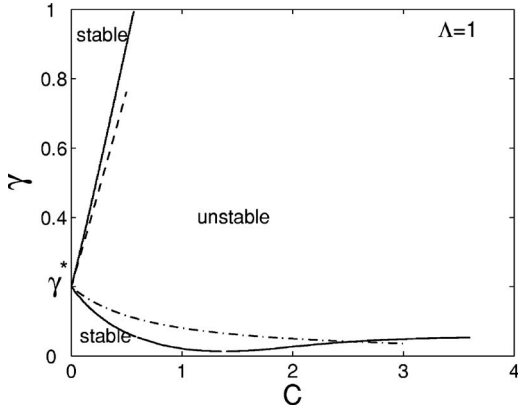


FIG. 2. The stability-instability region in the two-parameter space $\gamma-C$. The solid lines give the numerically obtained separatrices, while the dash-dotted and dashed ones the analytical approximations of Eqs. (15) and (16), respectively.

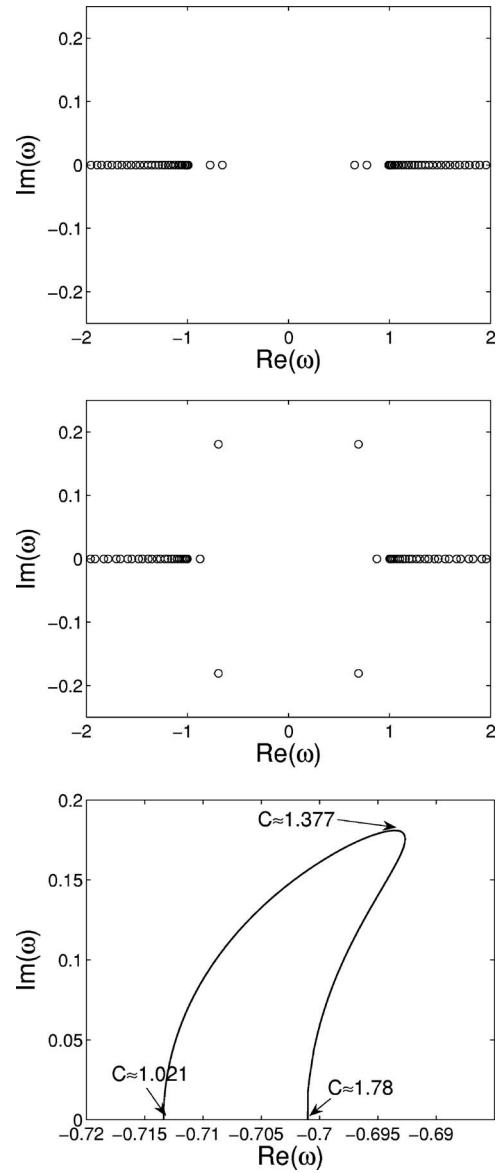


FIG. 3. The eigenvalue structure of a single-hump solitary wave for $\gamma=0.02$ and $C=1.0$ (top panel), as well as $C=1.4$ (middle panel). The bottom panel shows the trajectory of one of the unstable eigenvalues as C changes.

dash-dotted lines give the analytical prediction for the stability range as obtained by the conditions of collision of the phase mode eigenfrequency with the phonon band from Eqs. (15) and (16). Notice that this instability starts out at γ^* at the AC limit and expands into an instability band, as the phonon band of Eq. (14) itself expands for increasing C . We observe that the prediction of Eq. (16) is in very good agreement with the numerical observations for the occurrence of the instability point. This is because the collision typically occurs indeed with the upper band edge of the continuous spectrum (rather than with an eigenvalue bifurcating from it) and also typically the collision occurs for small C for which the analytical approximation of Eq. (12) is a very good approximation. On the other hand, the slightly less satisfactory agreement with the prediction of Eq. (15) occurs due to the collision with eigenvalues bifurcating from the lower edge of

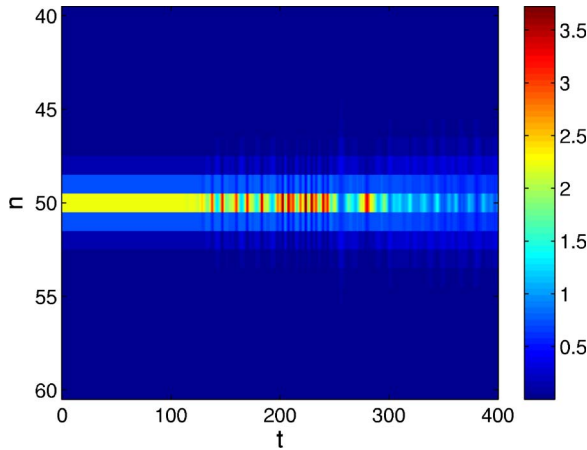


FIG. 4. (Color online) The spatio-temporal evolution of an unstable single-hump solitary wave at $\gamma=0.02$ and $C=1.4$. The contour plot of square modulus $|\phi_n|^2$ is shown.

the phonon band (see also Fig. 3 below) and also for relatively large C 's for which higher-order terms in the expansion of (12) should be expected to contribute.

Figure 3 illustrates the typical instability scenario for weak parametric drives ($\gamma=0.02$ in this figure). As C increases, the eigenvalue that is associated with the phase mode moves toward the phonon band of linear excitations (top panel). Eventually for $C \approx 1.021$, it collides with an eigenvalue pair that has bifurcated from the lower band edge. Due to the opposite Krein signature of these eigenvalues, their collision leads to an oscillatory instability and the bifurcation of a complex quartet of eigenvalues (middle panel). The Krein signature denotes the curvature of the energy surface associated with a given eigendirection around a stationary state—for a relevant discussion see, e.g., [13] and Eq. (23) therein for a definition; similar definitions arise in Eq. (5) of [15] or Eq. (14) of [16]. Eventually, as is shown in the bottom panel, the eigenfrequencies return to the real axis to restabilize the configuration for $C > 1.78$.

One can also notice from Fig. 2 that there is a minimum γ_m below which the soliton is stable all the way to the continuum limit. Numerically, $\gamma_m \approx 0.0135$. Unfortunately, since

γ_m occurs for large values of C (i.e., for $C > 1$), it cannot be predicted analytically by our expression γ_{cr}^1 (which is no longer valid in that regime).

We now turn to the examination of the dynamical behavior of the unstable solutions obtained above. The direct numerical evolution of an unstable solution of Eq. (1) is shown in Fig. 4. We have confirmed that this dynamics is typical of the unstable parameter range. The figure shows that eventually the solution becomes subject to the oscillatory instability that was illustrated in Fig. 3 and is ultimately destroyed completely. This may also be expected on the basis of the fact that this is the fundamental coherent structure solution and for the same parameter set there appears to be no other stable dynamical state (other than $\phi_n=0$) to which the initial condition may transform.

IV. CONCLUSIONS

In this Brief Report, we visited the topic of parametrically driven lattices of the NLS type. We have shown that the dynamics of these lattices is considerably different than those of the regular DNLS equation. This is due to the driving-induced bifurcation of the phase mode (associated with the gauge invariance of the NLS equation). Collision of this mode with eigenfrequencies stemming from the phonon band leads to a wide parametric regime of instabilities of the fundamental solitary wave in this model. Our perturbative analysis captures quite accurately the relevant eigenvalue (especially for weak couplings) and provides a fair estimate of the instability threshold in the parameter-space of the system. The result of the ensuing oscillatory instability is the destruction of the fundamental soliton, a feature absent from the regular DNLS model (where this solution is stable for all parameter values).

It would be interesting to expand the present considerations to other variants of the discrete parametrically driven model such as its higher-dimensional analogs, the defocusing case, or also damped variants of these lattice models. Such considerations are currently under study.

P.G.K. acknowledges support from NSF-DMS and CAREER and stimulating discussions with M. Agrotis at the early stages of this project.

- [1] S. Aubry, *Physica D* **103**, 201 (1997); S. Flach and C. R. Willis, *Phys. Rep.* **295**, 181 (1998); P. G. Kevrekidis, K. O. Rasmussen, and A. R. Bishop, *Int. J. Mod. Phys. B* **15**, 2833 (2001).
- [2] D. N. Christodoulides, F. Lederer, and Y. Silberberg, *Nature (London)* **424**, 817 (2003); Yu. S. Kivshar and G. P. Agrawal, *Optical Solitons: From Fibers to Photonic Crystals* (Academic Press, San Diego, 2003).
- [3] P. G. Kevrekidis and D. J. Frantzeskakis, *Mod. Phys. Lett. B* **18**, 173 (2004); V. V. Konotop and V. A. Brazhnyi, *ibid.* **18**, 627 (2004); P. G. Kevrekidis *et al.*, *ibid.* **18**, 1481 (2004).
- [4] M. Peyrard, *Nonlinearity* **17**, R1 (2004).
- [5] D. N. Christodoulides and R. I. Joseph, *Opt. Lett.* **13**, 794 (1988).
- [6] A. Trombettoni and A. Smerzi, *Phys. Rev. Lett.* **86**, 2353 (2001).
- [7] C. Sulem and P. L. Sulem, *The Nonlinear Schrödinger Equation* (Springer-Verlag, New York, 1999).
- [8] Yu. S. Kivshar and D. K. Campbell, *Phys. Rev. E* **48**, 3077 (1993).
- [9] T. Kapitula and P. Kevrekidis, *Nonlinearity* **14**, 533 (2001).
- [10] N. V. Alexeeva, I. V. Barashenkov, and D. E. Pelinovsky, *Nonlinearity* **12**, 103 (1999); I. V. Barashenkov and E. V. Zemlyanaya, *Phys. Rev. Lett.* **83**, 2568 (1999); I. V. Barashenkov, S. R. Woodford, and E. V. Zemlyanaya, *ibid.* **90**, 054103 (2003).
- [11] N. V. Alexeeva, I. V. Barashenkov, and G. P. Tsironis, *Phys. Rev. Lett.* **84**, 3053 (2000).
- [12] Yu. S. Kivshar and M. Peyrard, *Phys. Rev. A* **46**, 3198 (1992).
- [13] M. Johansson and S. Aubry, *Phys. Rev. E* **61**, 5864 (2000).
- [14] I. V. Barashenkov and Yu. S. Smirnov, *Phys. Rev. E* **54**, 5707 (1996).
- [15] D. V. Skryabin, *Phys. Rev. E* **64**, 055601 (2001).
- [16] A. V. Gorbach and M. Johansson, *Phys. Rev. E* **67**, 066608 (2003).